

Supplementary for

The A-site deficiency range identified for in-situ exsolution from $(\text{La}_{0.4}\text{Sr}_{0.6})_{1-\alpha}\text{Ti}_{0.95}\text{Ni}_{0.05}\text{O}_{3\pm\delta}$ electrodes for SOFC and SOEC.

Yao Jiang^{a,b}, Chengyu Li^c, Haonan Huang^a, Cairong Jiang^a, Yongjin Chen^{c*}, Yali Yao^{b,d}, Jianjun Ma^{a*}

^a School of Materials Science and Engineering, Sichuan University of Science and Engineering,

Zigong, Sichuan, 643000, PR China

^b Institute for the Development of Energy for African Sustainability (IDEAS), University of South

Africa, cnr Christiaan de Wet & Pioneer Roads, Roodepoort, Private Bag X6, 1710, South Africa

^c Center for High Pressure Science and Technology Advanced Research (HPSTAR), Beijing, 100094, P.

R. China

^d Zhijiang College of Zhejiang University of Technology, Shaoxing, Zhejiang, 312030, P. R. China

Corresponding Author

JM-School of Materials Science and Engineering, Sichuan University of Science and Engineering,
Zigong, Sichuan, 643000, PR China; ORCID ID:0000-0002-0016-6313; E-mail: jjma@suse.edu.cn;

Tel: +86 15808219478

YC-Center for High Pressure Science and Technology Advanced Research (HPSTAR), Beijing,

100094, P. R. China; E-mail: yongjin.chen@hpstar.ac.cn;

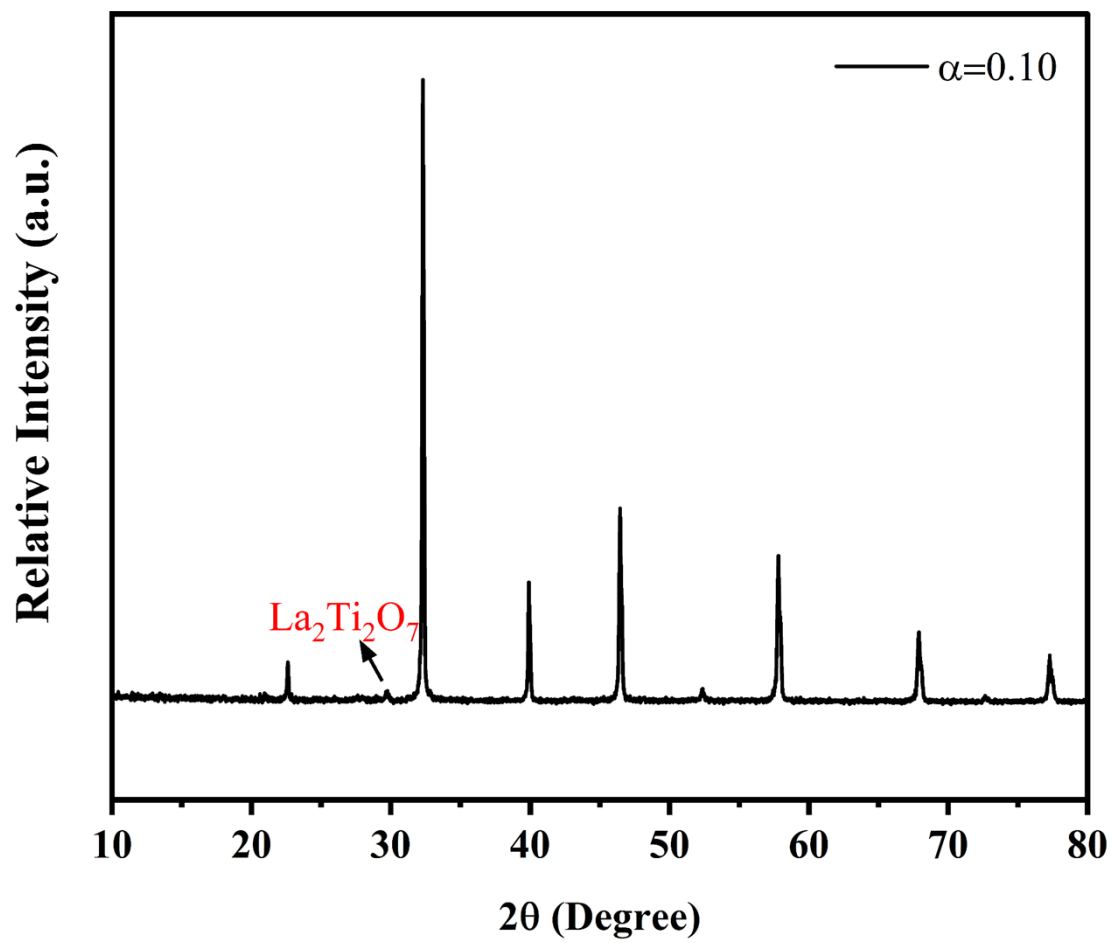


Fig. S1 XRD patterns of LSTN of $\alpha=0.10$.

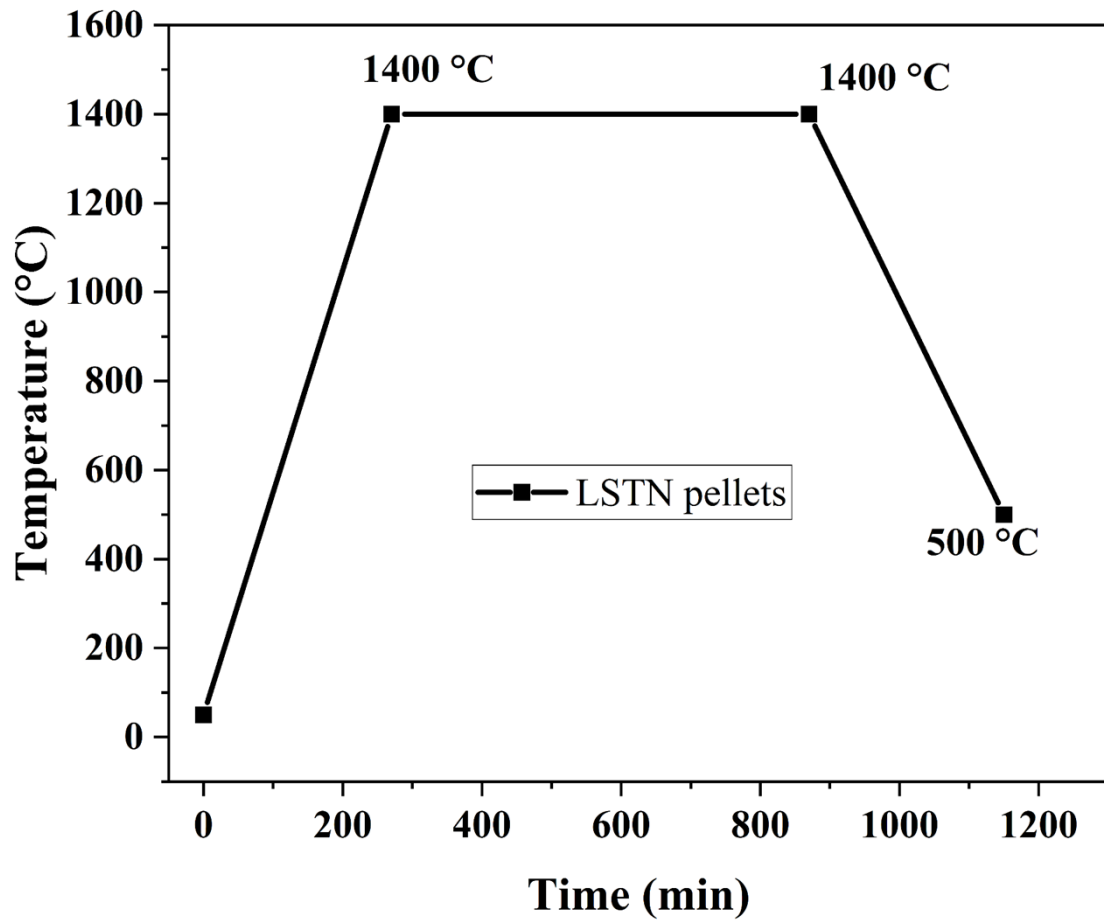


Fig. S2 Uniform sintering curves on samples characterised by sintering properties and conductivity of LSTN with different deficiencies.

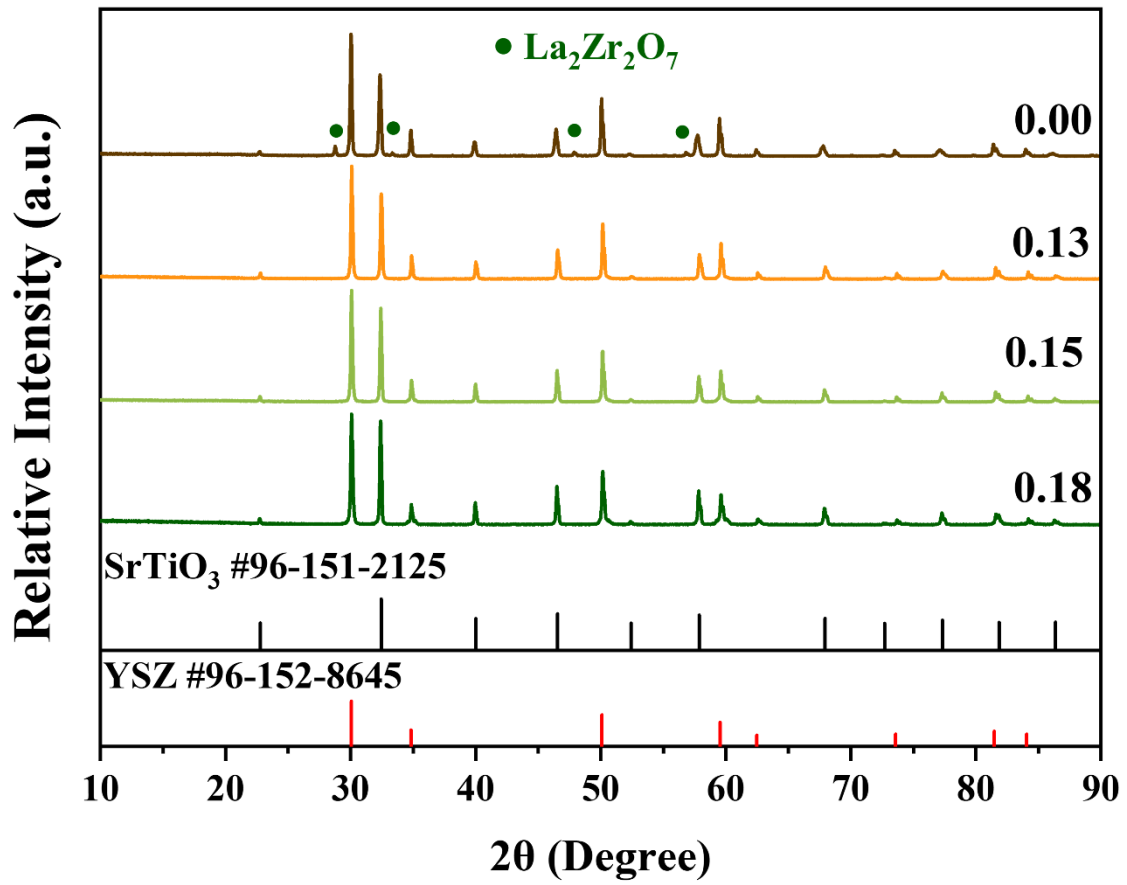


Fig. S3 XRD patterns of LSTN and YSZ mixed powders calcined at 1200 °C for 10 h

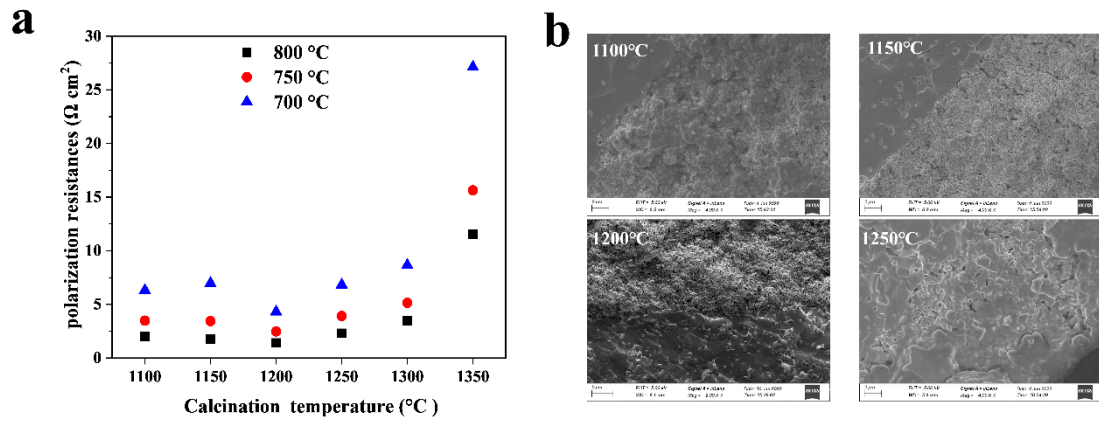


Fig. S4 Electrochemical performance optimization of LSTN-46-13 electrode at different calcination temperatures. (a) Polarization resistance

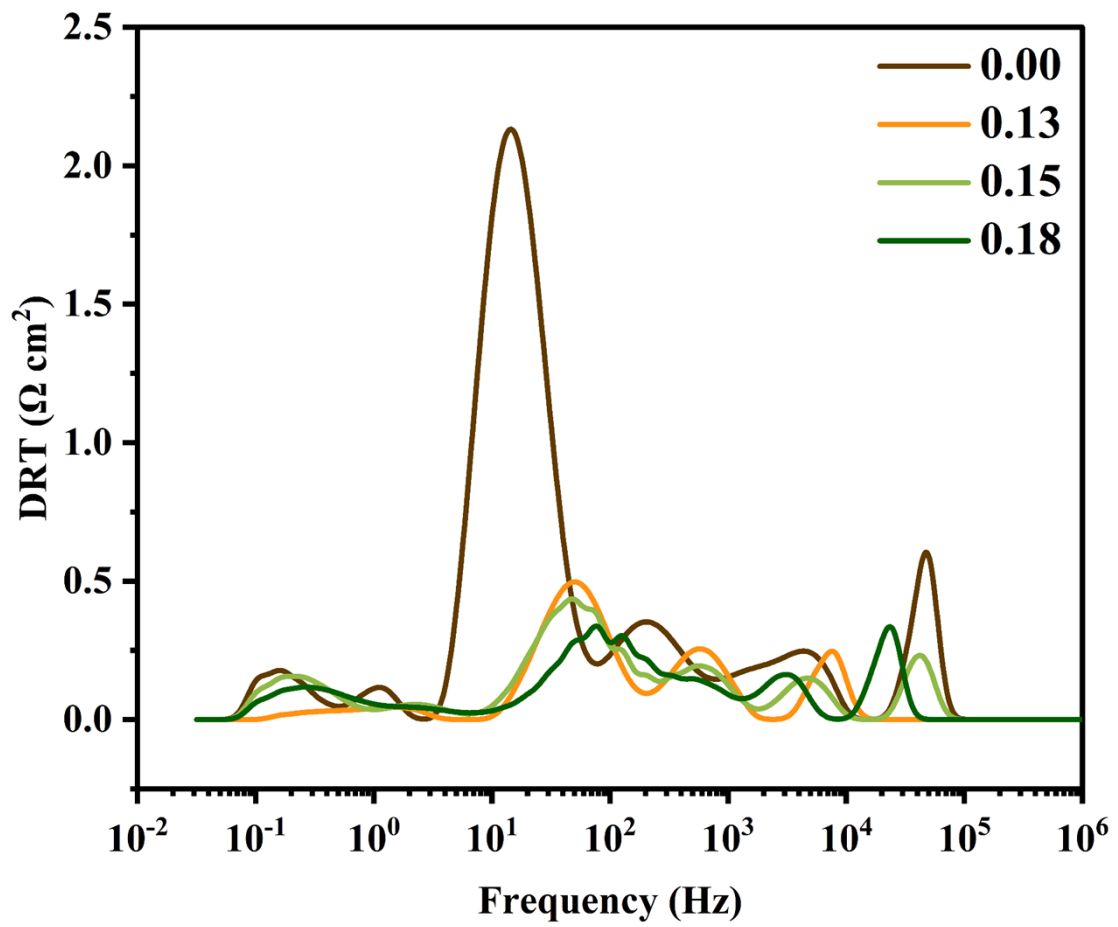


Fig. S5 DRT analysis of impedance spectra data for the LSTN cells at 800 °C

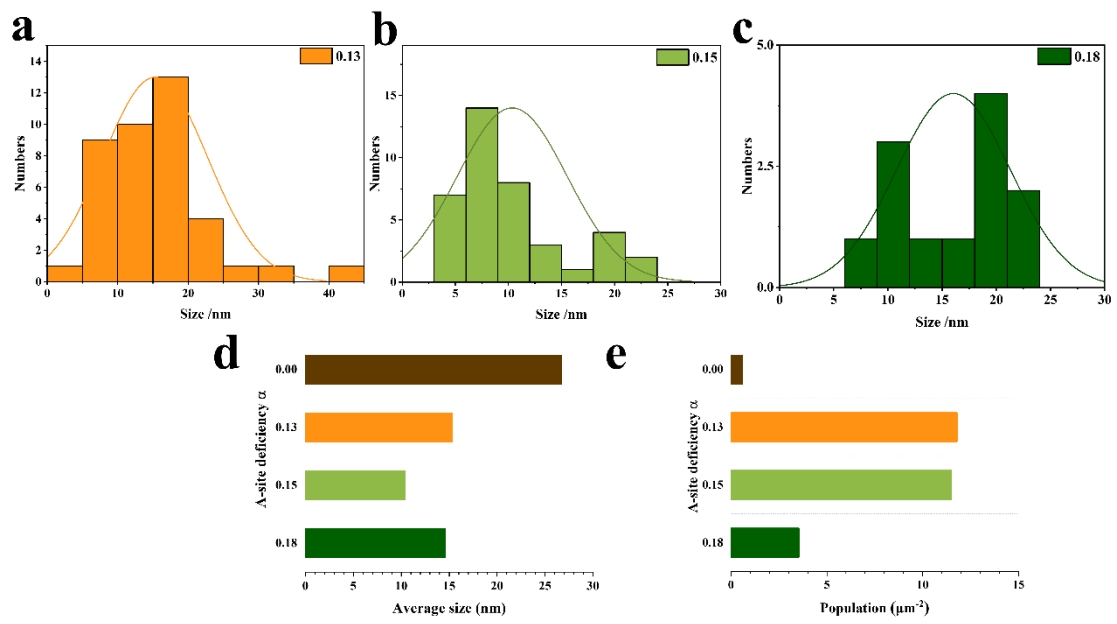


Fig. S6 Distributions of Ni NPs in LSTN samples after SOFC test (α value from 0.13 to 0.18), (a) $\alpha = 0.13$, (b) $\alpha = 0.15$, (c) $\alpha = 0.18$. (d) The average size of Ni nanoparticles. (e) The population of Ni nanoparticles.

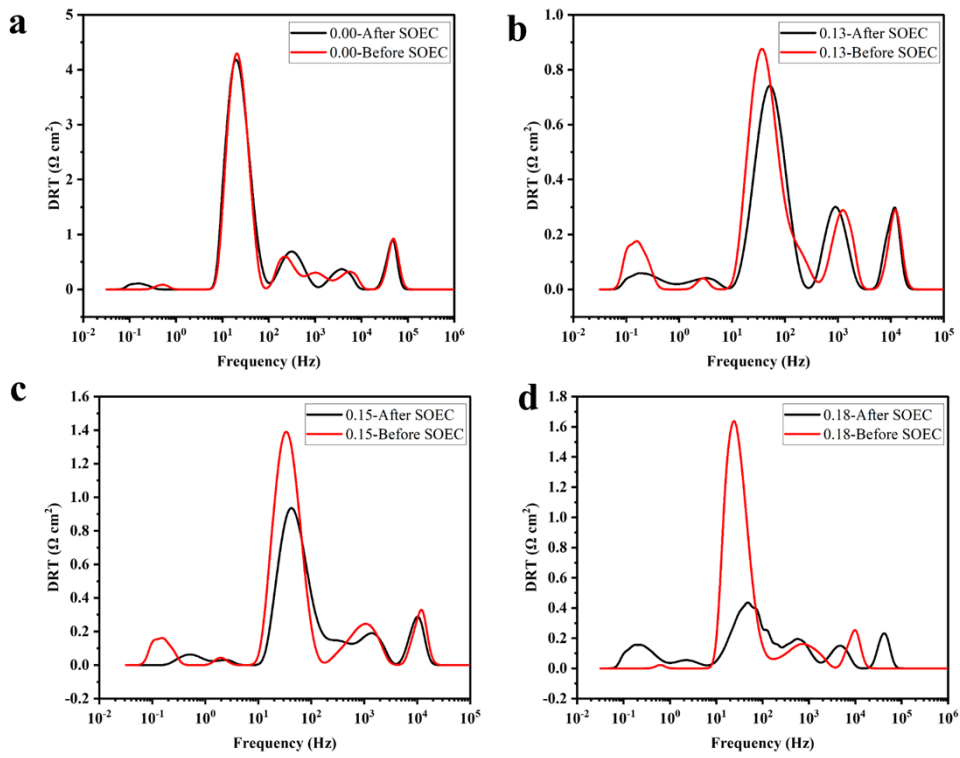


Fig. S7 DRT analysis of impedance spectra data before and after SOEC test for LSTN with different A site deficiency (α value from 0.00 to 0.18), (a) $\alpha = 0.00$, (b) $\alpha = 0.13$, (c) $\alpha = 0.15$, (d) $\alpha = 0.18$.

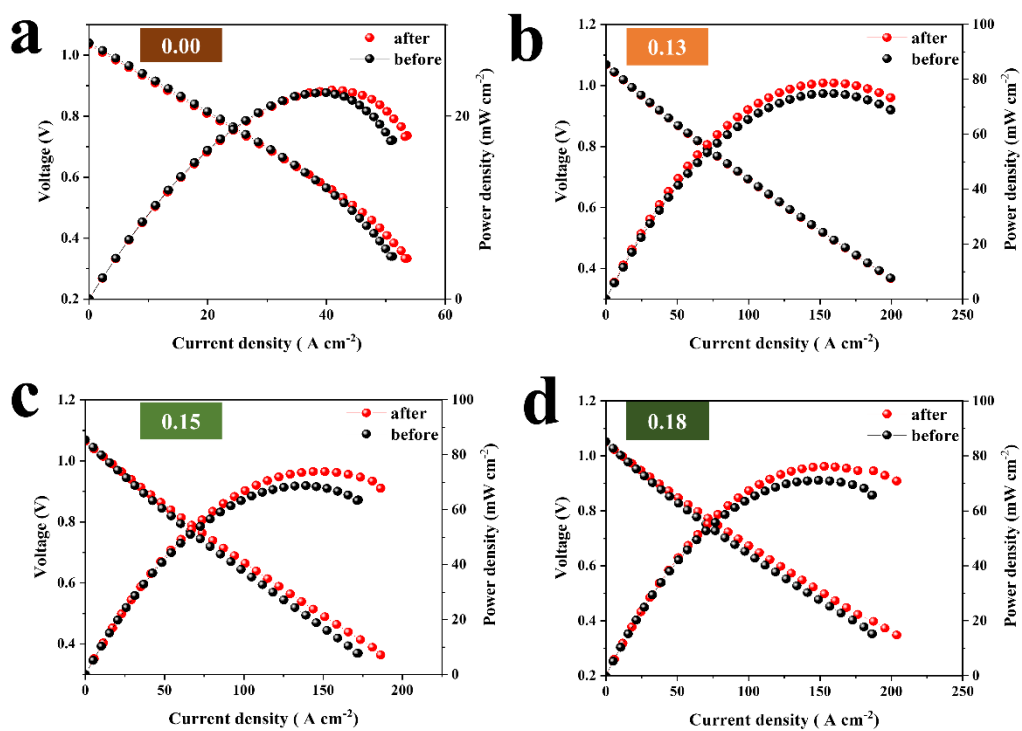


Fig. S8 The current–voltage curves (800 ° C, wet H_2) before and after SOEC test for LSTN with different A site deficiency (α value from 0.00 to 0.18), (a) $\alpha = 0.00$, (b) $\alpha = 0.13$, (c) $\alpha = 0.15$, (d) $\alpha = 0.18$.

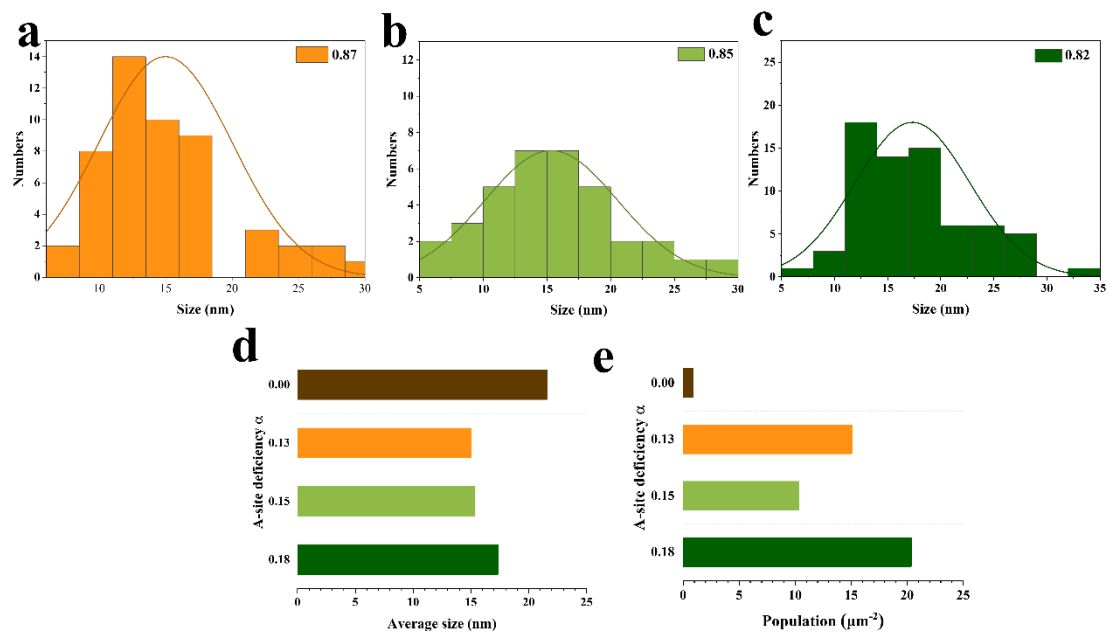


Fig. S9 The distributions of Ni NPs in LSTN samples after SOEC test (α value from 0.13 to 0.18), (a) $\alpha = 0.13$, (b) $\alpha = 0.15$, (c) $\alpha = 0.18$. (d) The average diameter of Ni nanoparticles. (e) The population of Ni nanoparticles.

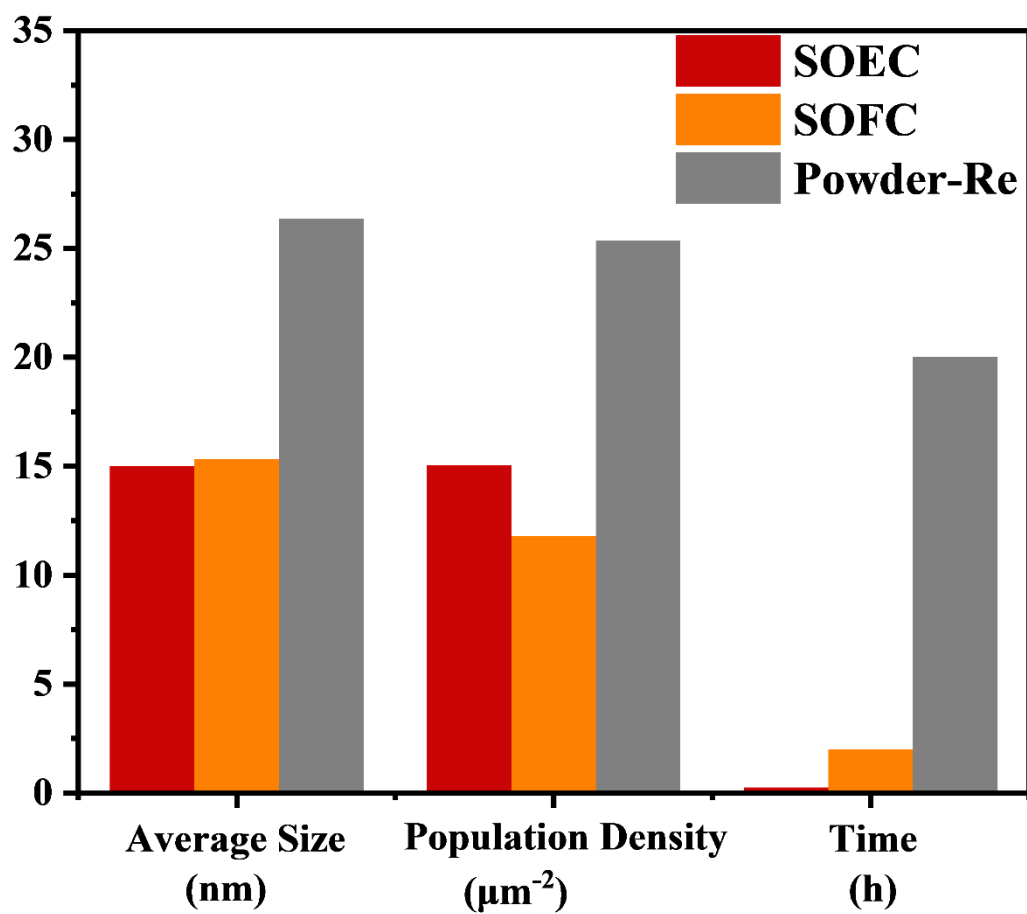


Fig. S10 Comparison of size, number and treatment time of Ni nanoparticles from different exsolution processes.